Journal of Power Sources 226 (2013) 210–218

Contents lists available at SciVerse ScienceDirect

Journal of Power Sources

journal homepage: www.elsevier.com/locate/jpowsour

Properties and application of ether-functionalized trialkylimidazolium ionic liquid electrolytes for lithium battery

Yide Jin [a], Shaohua Fang [a,*], Ming Chai [a,b,c], Li Yang [a,*], Kazuhiro Tachibana [c], Shin-ichi Hirano [b]

[a] School of Chemistry and Chemical Technology, Shanghai Jiaotong University, Shanghai 200240, China
[b] Hirano Institute for Materials Innovation, Shanghai Jiaotong University, Shanghai 200240, China
[c] Department of Chemistry and Chemical Engineering, Faculty of Engineering, Yamagata, University, Yamagata 992-8510, Japan

HIGHLIGHTS

- New trialkylimidazolium ILs are used as electrolytes for lithium battery.
- Ether group in IL cation can have effect on properties of IL electrolyte.
- Li/LiFePO$_4$ cells using these IL electrolytes have good electrochemical performance.

ARTICLE INFO

Article history:
Received 15 August 2012
Received in revised form
30 September 2012
Accepted 25 October 2012
Available online 2 November 2012

Keywords:
Lithium battery
Ionic liquid
Electrolyte
Functionalized cation

ABSTRACT

Six low-viscosity ionic liquids based on trialkylimidazolium cation with one or two ether groups and $TFSA^-$ anion are used as new electrolytes for lithium battery, and compared with three typical trialkylimidazolium ILs without ether group. It is found that ether group in trialkylimidazolium cation can have an obvious effect on properties of electrolyte and performances of lithium battery. Introducing of ether group into trialkylimidazolium cation can be benefit for lithium redox behavior on Ni electrode, and affect passivation layer between IL electrolyte and lithium metal. Li/LiFePO$_4$ cells using these ether-functionalized IL electrolytes without additive have good battery performance, and IM(2o1)1(2o2)-TFSA electrolyte owns better rate property.

1. Introduction

Over the past decade, ionic liquids (ILs) have attracted growing interests as safe electrolytes for lithium battery, due to their negligible vapor pressure, non-flammability, good thermal and electrochemical stability, and high conductivity [1–3]. For example, quaternary ammonium, pyrrolidinium, piperidinium, phosphonium and guanidinium ILs have been reported as new electrolytes for lithium battery [4–17].

1,3-dialkylimidazolium ILs are most widely studied ILs for different applications, especially 1-ethyl-3-methylimidazolium ILs, due to easy preparation and low viscosity [3,18,19]. However, the presence of an active hydrogen at the C-2 position of 1,3-dialkylimidazolium ring can cause the problem of electrochemical instability, which restricts the usage in lithium battery [20–22]. 1,2,3-trialkylimidazolium ILs are acquired after substituting the hydrogen at the C-2 position in 1,3-dialkylimidazolium ring by an alkyl group, and the electrochemical stabilities can be improved obviously, which makes these ILs to become very attractive electrolytes for lithium battery, though their viscosities increase slightly with the increasing of cation size. And 1,2-dimethyl-3-propylimidazolium bis(trifluoromethanesulfonyl)imide (IM113-TFSA) and 1,2-dimethyl-3-amylimidazolium bis(trifluoromethanesulfonyl)imide (IM115-TFSA) have been applied as IL electrolytes for lithium battery [23–25].

Currently, functionalized IL is a very noticeable topic in the field of IL research. Introducing different functional groups, such as amine, amide, nitrile, ether, alcohol, ester functionalities into IL cations, the physicochemical and electrochemical properties of ILs can be observably tuned, and providing more choices for applications of ILs [26–35]. In comparison to other functional groups, ether group can reduce the viscosities and melting points of ILs without resulting the obvious degradation of electrochemical stability [33–37]. One ether group has already been introduced into imidazolium, quaternary

* Corresponding authors. Tel.: +86 21 54748917; fax: +86 21 54741297.
E-mail addresses: housefang@sjtu.edu.cn (S. Fang), liyangce@sjtu.edu.cn (L. Yang).

0378-7753/$ – see front matter © 2012 Elsevier B.V. All rights reserved.
http://dx.doi.org/10.1016/j.jpowsour.2012.10.076

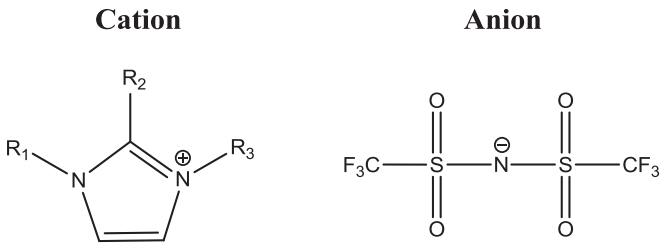

	Abbreviation
R_1=R_2=CH_3, R_3=CH_2CH_3	IM112-TFSA
R_1=R_2=CH_3, R_3=$CH_2CH_2CH_3$	IM113-TFSA
R_1=R_2=CH_3, R_3=$CH_2CH_2CH_2CH_3$	IM114-TFSA
R_1=CH_2CH_3, R_2=CH_3, R_3=$CH_2CH_2OCH_3$	IM(2o1)12-TFSA
R_1=CH_2CH_3, R_2=CH_3, R_3=$CH_2CH_2OCH_2CH_3$	IM(2o2)12-TFSA
R_1=CH_3, R_2=CH_2CH_3, R_3=$CH_2CH_2OCH_3$	IM(2o1)21-TFSA
R_1=CH_3, R_2=CH_2CH_3, R_3=$CH_2CH_2OCH_2CH_3$	IM(2o2)21-TFSA
R_1=$CH_2CH_2OCH_3$, R_2=CH_3, R_3=$CH_2CH_2OCH_2CH_3$	IM(2o1)1(2o2)-TFSA
R_1=$CH_2CH_2OCH_2CH_3$, R_2=CH_3, R_3=$CH_2CH_2OCH_2CH_3$	IM(2o2)1(2o2)-TFSA

Fig. 1. Structures of ether-functionalized trialkylimidazolium ILs and trialkylimidazolium ILs without ether group used in this study.

ammonium and phosphonium, pyrrolidinium, piperidinium, morpholinium, guanidinium, sulfonium and pyrazolium cations [38–45]. Some electrolytes for lithium battery have been found from these ILs with one ether group, such as *N*,*N*-diethyl-*N*-methyl-*N*-(2-methoxyethyl) ammonium bis(trifluoromethanesulfonyl) imide (DEME-TFSA), *N*-methoxyethyl-*N*-methylpyrrolidinium TFSA (PY1(2o1)-TFSA), triethyl(2-methoxyethyl) phosphonium TFSA (P222(2o1)-TFSA) and *N*-methyl-*N*-(2-methoxyethyl)-tetramethylguanidinium TFSA (1g1(2o1)-TFSA) [46–52]. Recently, several kinds of ILs based on cations with two or more ether groups have also been reported, and some pyrrolidinium, piperidinium and guanidinium ILs with two ether groups, and quaternary ammonium ILs with three or more ether groups have also been applied as electrolytes for lithium battery [53–57].

Recently, our group has synthesized a series of ILs based on trialkylimidazolium cations with one or two ether groups and $TFSA^-$ anion, and some of these ILs had low viscosity [58]. In the present study, six ether-functionalized trialkylimidazolium ILs with viscosity lower than 75 cP were chosen as new electrolytes for lithium battery, and compared with three typical trialkylimidazolium ILs without ether group. And the structures of these ILs were shown in Fig. 1. Viscosity, conductivity, behavior of lithium redox, chemical stability against lithium metal, and

Table 1
Viscosity and conductivity of the nine ILs without and with 0.6 mol kg^{-1} of LiTFSA at 25 °C.

	ILs without LiTFSA		ILs with LiTFSA	
	Viscosity [58]/ mPa s	Conductivity [58]/mS cm^{-1}	Viscosity/ mPa s	Conductivity/ mS cm^{-1}
IM112-TFSA	84.6	2.75	195.1	1.24
IM113-TFSA	61.1	3.99	157.5	1.84
IM114-TFSA	89.7	2.22	223.4	0.95
IM(2o1)12-TFSA	57.4	3.03	132.5	1.32
IM(2o2)12-TFSA	54.4	2.70	129.1	1.28
IM(2o1)21-TFSA	67.2	2.06	191.6	0.77
IM(2o2)21-TFSA	71.6	2.27	197.5	0.84
IM(2o1)1(2o2)-TFSA	62.5	1.84	198.8	0.80
IM(2o2)1(2o2)-TFSA	70.2	1.62	205.8	0.70

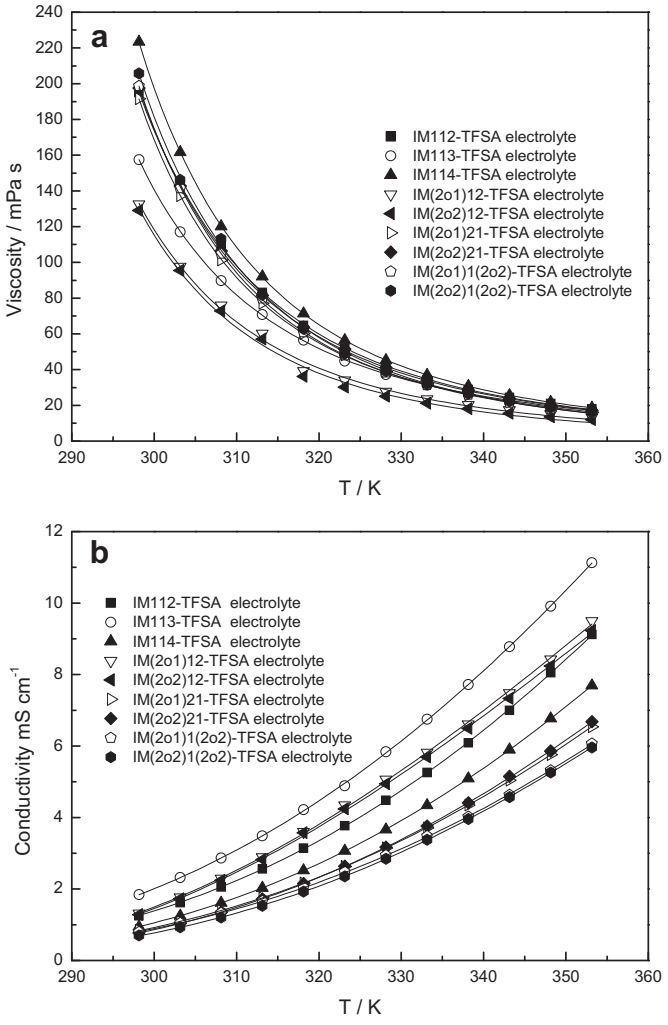

Fig. 2. Change of (a) viscosity and (b) conductivity with temperature for these IL electrolytes.

Table 2
VTF equation parameters of viscosity for the IL electrolytes.

IL electrolytes	η_0 (mPa s)	B (K)	T_0 (K)	R^2
IM112-TFSA	0.100 (±15%)	895.2 (±5%)	179.9 (±2%)	0.999
IM113-TFSA	0.256 (±12%)	670.5 (±6%)	193.8 (±1%)	0.999
IM114-TFSA	0.116 (±8%)	850.6 (±2%)	185.8 (±1%)	0.999
IM(2o1)12-TFSA	0.276 (±9%)	654.8 (±3%)	203.6 (±1%)	0.999
IM(2o2)12-TFSA	0.297 (±8%)	646.5 (±2%)	205.7 (±1%)	0.999
IM(2o1)21-TFSA	0.193 (±10%)	682.4 (±4%)	199.2 (±1%)	0.999
IM(2o2)21-TFSA	0.168 (±11%)	741.9 (±4%)	193.1 (±1%)	0.999
IM(2o1)1(2o2)-TFSA	0.108 (±12%)	807.8 (±4%)	190.6 (±1%)	0.999
IM(2o2)1(2o2)-TFSA	0.089 (±14%)	1018.5 (±5%)	176.0 (±1%)	0.999

The percentage standard errors for η_0, B and T_0 have been included, and R^2 is the VTF fitting coefficient.

charge–discharge characteristics of lithium batteries, were investigated for these IL electrolytes, and it was found that ether group in trialkylimidazolium cation could have an obvious effect on the properties of electrolyte and the performances of lithium battery.

2. Experimental

The structures of six ether-functionalized trialkylimidazolium ILs and three trialkylimidazolium ILs without ether group used in this study were shown in Fig. 1, and the nine ILs were prepared according to the our reported methods [58]. These ILs were dried under high vacuum for more than 48 h at 105 °C before using. The water content of the dried ILs was detected by a moisture titrator (Metrohm 73 KF coulometer) basing on Karl-Fischer method, and the value was bellow 50 ppm. Then 0.6 mol kg^{-1} of LiTFSA (kindly provided by Morita Chemical Industries Co., Ltd.), were added to the dried ILs. And this procedure was carried out in an argon-filled glove box ($[O_2] < 1$ ppm, $[H_2O] < 1$ ppm).

The viscosities of IL electrolytes were tested with viscometer (DV-III ULTRA, Brookfield Engineering Laboratories, Inc.), and the conductivities were got from DDS-11A conductivity meter. The electrochemical windows of the ILs were tested by linear sweep voltammograms (LSV, scan rate 10 mV s^{-1}) in glove box. The working electrode was glassy carbon disk (3 mm diameter), and lithium metal was used as both counter and reference electrodes. The glassy carbon electrode was polished with alumina paste ($d = 0.1$ μm), and the polished electrode was washed with deionized water and dried under vacuum. The LSV tests were performed by CHI660D electrochemistry workstation at room temperature.

The stability of the IL electrolytes against lithium metal at room temperature was investigated by monitoring the time evolution of the impedance response for a symmetric Li/IL electrolyte/Li coin cell with the borosilicate glass separator (GF/A, Whatman), and the impedance responses were measured by using CHI660D electrochemistry workstation (100 KHz–100 mHz; applied voltage 5 mV).

The plating and stripping behaviors of lithium in the IL electrolytes was determined by using cyclic voltammograms (CV, scan rate 10 mV s^{-1}) method in the glove box. The nickel disk (2 mm diameter) was used as the working electrode and lithium metal was used as both counter and reference electrodes. The nickel electrode was polished in the usage of alumina paste ($d = 0.1$ μm). And the Ni electrode was washed by deionized water then dried under vacuum. The CV tests were performed by CHI660D electrochemistry workstation at room temperature (25 °C).

Li/$LiFePO_4$ coin cell was used to evaluate the performances of the IL electrolytes in lithium battery applications. Lithium foil (battery grade) was used as a negative electrode and the positive electrode was fabricated by spreading the mixture of $LiFePO_4$, acetylene black and PVDF (firstly dissolved in *N*-methyl-*N*-2-pyrrolidone) with a weight ratio of 8:1:1 on aluminum current collector (battery use). Loading of active materials was about ca. 1.5–2.0 mg cm^{-2} and this electrode was used without pressing. The separator was glass filter made of borosilicate glass (GF/A, Whatman). Cell was assembled in the glove box, and all the components of cell were dried under vacuum before using. Cell performances were examined by the charge–discharge (C–D) cycling tests using a CT2001A cell test instrument (LAND Electronic Co., Ltd.) at 25 °C and at different current rates (0.1 C–2.5 C), current was determined by the theoretical capacity of 170 mAh g^{-1} for Li/$LiFePO_4$ cell. The cells were sealed and then stayed at room temperature for 4 h

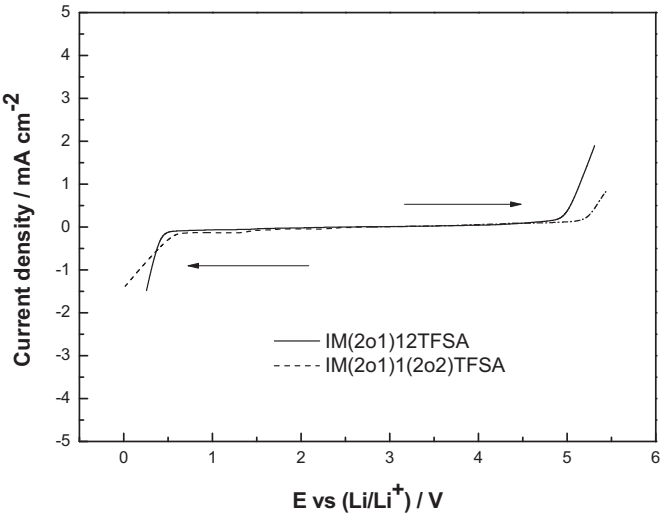

Fig. 3. Linear sweep voltammograms of IM(2o1)12TFSA and IM(2o1)1(2o2)TFSA at 25 °C. Working electrode: glassy carbon, counter electrode: Li, reference electrode: Li, scan rate: 10 mV s^{-1}.

Table 3
VTF equation parameters of conductivity for the IL electrolytes.

IL electrolytes	σ_0 (mS cm^{-1})	B (K)	T_0 (K)	R^2
IM112-TFSA	541.6 (±11%)	688.7 (±5%)	184.9 (±2%)	0.999
IM113-TFSA	491.7 (±13%)	647.0 (±6%)	182.4 (±2%)	0.999
IM114-TFSA	414.4 (±5%)	636.7 (±2%)	193.4 (±1%)	0.999
IM(2o1)12-TFSA	347.6 (±9%)	631.8 (±3%)	196.2 (±1%)	0.999
IM(2o2)12-TFSA	307.5 (±7%)	617.3 (±2%)	209.1 (±1%)	0.999
IM(2o1)21-TFSA	272.4 (±7%)	554.2 (±3%)	203.0 (±1%)	0.999
IM(2o2)21-TFSA	354.5 (±4%)	643.9 (±2%)	191.9 (±1%)	0.999
IM(2o1)1(2o2)-TFSA	368.2 (±13%)	686.4 (±5%)	186.1 (±2%)	0.999
IM(2o2)1(2o2)-TFSA	229.6 (±5%)	539.9 (±3%)	205.2 (±1%)	0.999

The percentage standard errors for σ_0, B and T_0 have been included, and R^2 is the VTF fitting coefficient.

Table 4
Cathodic and anodic limiting potentials (versus Li/Li^+) and electrochemical windows of various ILs determined at 25 °C.

ILs	Cathodic limiting potential	Anodic limiting potential	Electrochemical window (V)
	E versus (Li/Li^+)/V	E versus (Li/Li^+)/V	
IM112-TFSA	0.3	4.9	4.6
IM113-TFSA	0.3	4.9	4.6
IM114-TFSA	0.2	4.9	4.7
IM(2o1)12-TFSA	0.4	4.9	4.5
IM(2o2)12-TFSA	0.5	4.9	4.4
IM(2o1)21-TFSA	0.6	5.1	4.5
IM(2o2)21-TFSA	0.5	5.0	4.5
IM(2o1)1(2o2)-TFSA	0.6	5.2	4.6
IM(2o2)1(2o2)-TFSA	0.5	5.1	4.6

Working electrode: glassy carbon, counter electrode: Li, reference electrode: Li, scan rate: 10 mV s^{-1}, cut-off current density: 0.2 mA cm^{-2}.

before the performance tests. Constant current charge–discharge cycles were conducted between 2.0 and 4.0 V (vs. Li/Li^+). Charging included two processes: (1) constant current at a rate, cut-off voltage of 4.0 V; (2) constant voltage at 4.0 V, held for 1 h. And discharging had one process: constant current at the same rate, cut-off voltage of 2.0 V.

3. Results and discussion

3.1. Viscosity and conductivity of the IL electrolytes

The viscosities and conductivities at room temperature of the nine trialkylimidazolium ILs and their IL electrolytes with 0.6 mol kg^{-1} LiTFSA are listed in Table 1. Among the three trialkylimidazolium ILs without ether group, IM113TFSA owned the lowest viscosity of 61.1 mPa s. The viscosities of the six ether-functionalized trialkylimidazolium ILs in this study were in the range of 54.4–71.6 mPa s, and they could also belong to low-viscosity ILs. Compared with the other ILs, which had been used in lithium battery without additive, the viscosities of these ether-functionalized ILs were slightly higher than the EMI-FSA (bis(-fluorosulfonyl)imide) and P13-FSA, and obviously lower than PP13-TFSA, DEME-TFSA and several other quaternary ammonium-based ILs [6,7,59].

After lithium salt dissolved in the IL, the lithium ion with the higher positive charge density compared with the cation of IL

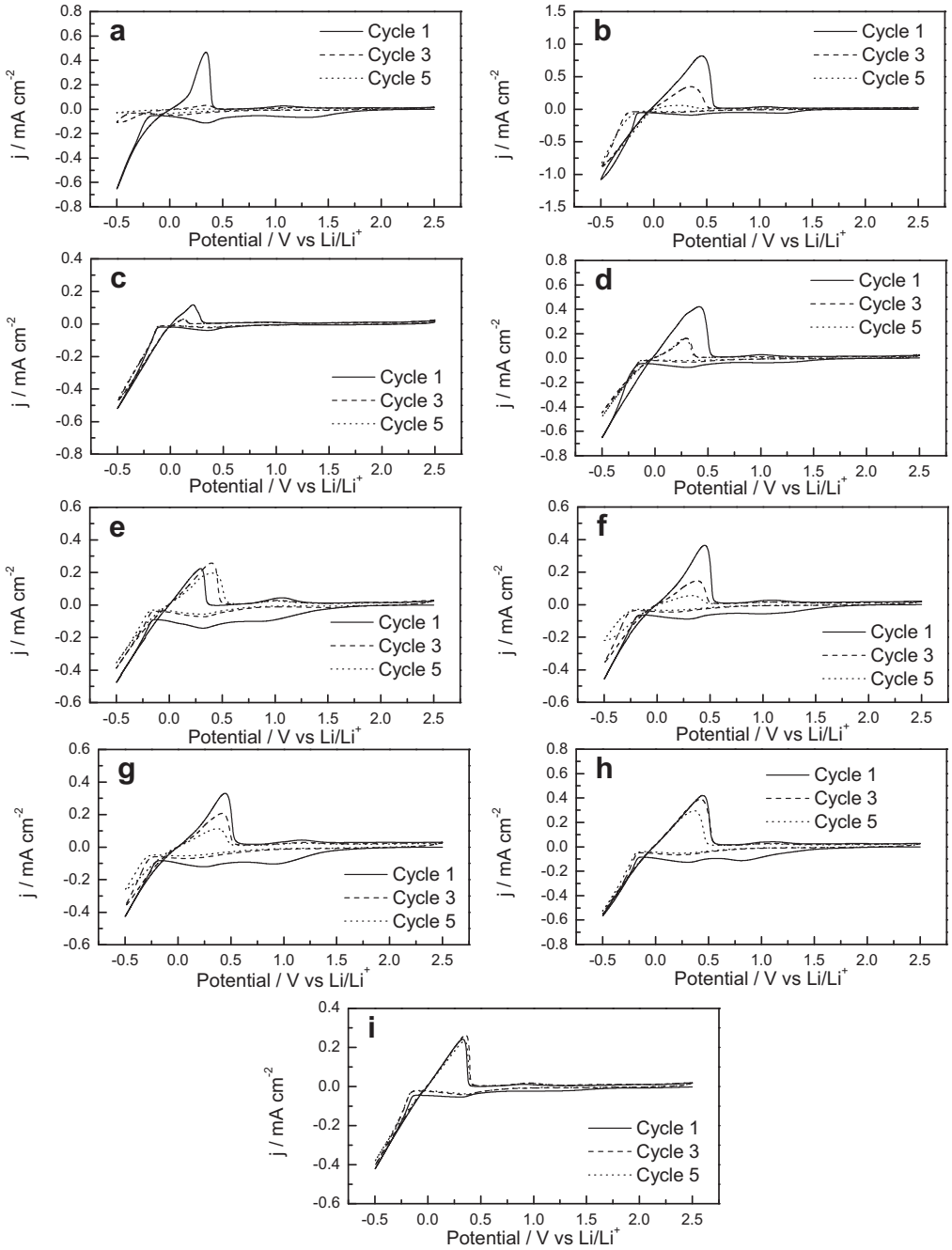

Fig. 4. Cyclic voltammograms of these IL electrolytes at 25 °C (−0.5 V–2.5 V versus Li/Li^+). (a) IM112-TFSA electrolyte, (b) IM113-TFSA electrolyte, (c) IM114-TFSA electrolyte, (d) IM(2o1)12-TFSA electrolyte, (e) IM(2o2)12-TFSA electrolyte, (f) IM(2o1)21-TFSA electrolyte, (g) IM(2o2)21-TFSA electrolyte, (h) IM(2o1)1(2o2)-TFSA electrolyte, (i) IM(2o2)1(2o2)-TFSA electrolyte. Working electrode, Ni; counter electrode, Li; reference electrode, Li; scan rate, 10 mV s^{-1}.

would form ionic clusters with anions, which would result in stronger electrostatic interactions among the ionic species in the IL electrolyte and higher viscosity [60–62]. Like some other ILs, such as quaternary ammonium ILs, pyrrolidinium and piperidinium ILs [48,63,64], the viscosity of these trialkylimidazolium IL electrolytes increased obviously after adding the LiTFSA salt into the ILs. Usually, if the ILs own lower viscosity, their IL electrolytes also show smaller value of viscosity. For example, for the three trialkylimidazolium ILs without ether group, the IL viscosity increased as followed: IM113-TFSA (61.1 mPa s) < IM112-TFSA (84.6 mPa s) < IM114-TFSA (89.7 mPa s), and their IL electrolyte viscosity increasing order was IM113-TFSA electrolyte (157.5 mPa s) < IM112-TFSA electrolyte (195.1 mPa s) <IM114-TFSA electrolyte (223.4 mPa s). However, for the six ether-functionalized ILs, the viscosity increasing order of these IL electrolytes was not consistent with the pure ILs. For instance, the viscosity of IM(2o1)1(2o2)-TFSA (62.5 mPa s) was lower than IM(2o1)21-TFSA (67.2 mPa s), and the viscosity of IM(2o1)1(2o2)-TFSA electrolyte (198.8 mPa s) was higher than IM(2o1)21-TFSA electrolyte (191.6 mPa s). It indicated that two ether groups in trialkylimidazolium cation could cause the more obvious increasing of viscosity for IL electrolyte.

The temperature dependence of viscosity was investigated for all the nine IL electrolytes over the temperature range 25–80 °C, as shown in Fig. 2(a), and the $\eta(T)$ behavior was fitted by a Vogel–Tammann–Fulcher (VTF) Equation (1):

$$\eta = \eta_0 \exp\left(\frac{B}{T - T_0}\right) \quad (1)$$

where η_0 (mPa s), B (K) and T_0 (K) are adjustable parameters. The resultant best-fit η_0 (mPa s), B (K) and T_0 (K) parameters for all the IL electrolytes are given in Table 2 along with the corresponding fitting coefficient R^2 values. According to Fig. 2(a) and the values of R^2 in Table 2, the viscosity of these IL electrolytes were well fitted by the VTF model over the temperature range studied. For IM112-TFSA, IM113-TFSA and IM114-TFSA electrolytes, the three parameters did not show direct relationship with their viscosities at room temperature. For the six ether-functionalized trialkylimidazolium IL electrolytes, the IL electrolyte with higher viscosity at room temperature owned bigger B value, smaller η_0 and smaller T_0 values.

After adding lithium salts into these trialkylimidazolium ILs, the conductivities decreased obviously along with the increasing of viscosities. In the nine trialkylimidazolium IL electrolytes, IM113-TFSA electrolyte owned the highest conductivity of 1.84 mS cm^{-1}. For the ether-functionalized IL electrolytes, two IL electrolytes had conductivity values higher than 1 mS cm^{-1}, and IM(2o1)12-TFSA electrolyte had the higher conductivity of 1.32 mS cm^{-1}.

Likewise, the temperature dependence of conductivity was also investigated for all the nine IL electrolytes over the temperature range 25–80 °C, as shown in Fig. 2(b), and the σ(T) behavior was fitted by a VTF Equation (2):

$$\sigma = \sigma_0 \exp\left(\frac{-B}{T - T_0}\right) \quad (2)$$

where σ_0 (mS cm^{-1}), B (K) and T_0 (K) are adjustable parameters of Equation (2). These three values and the VTF fitting coefficient (R^2) for them were calculated and listed in Table 3. The temperature dependence of conductivity was also very well fitted by the VTF model over the temperature range studied. And the σ_0, B and T_0 values did not show apparent relationship with their conductivities at room temperature for these nine IL electrolytes.

3.2. Electrochemical windows of these ILs and lithium redox in these IL electrolytes

The electrochemical stabilities of these trialkylimidazolium ILs were investigated by linear sweep voltammograms (LSV) using lithium metal as reference and counter electrode. And the LSV curves of two ILs at 25 °C are shown as examples in Fig. 3. The cathodic limiting potentials of IM(2o1)12-TFSA and IM(2o1)1(2o2)-TFSA were 0.4 V and 0.6 V versus Li/Li$^+$, and their anodic limiting potentials were about 4.9 V and 5.2 V versus Li/Li$^+$, so the electrochemical window were 4.5 V and 4.6 V respectively. The cathodic limiting potentials, anodic limiting potentials and electrochemical windows of these ILs are listed in Table 4. As already reported, introducing one or more ether groups into the cations of quaternary ammonium and cyclic quaternary ammonium ILs could reduce the electrochemical stability [33,34]. It could also be found that the electrochemical windows of ether-functionalized trialkylimidazolium ILs were slightly lower than the trialkylimidazolium ILs without ether group.

According to the cathodic limiting potentials of these trialkylimidazolium ILs, which were higher than 0 V versus Li/Li$^+$, it was possible that their IL electrolytes with 0.6 mol kg^{-1} LiTFSA might not allow the deposition of lithium ion without additives.

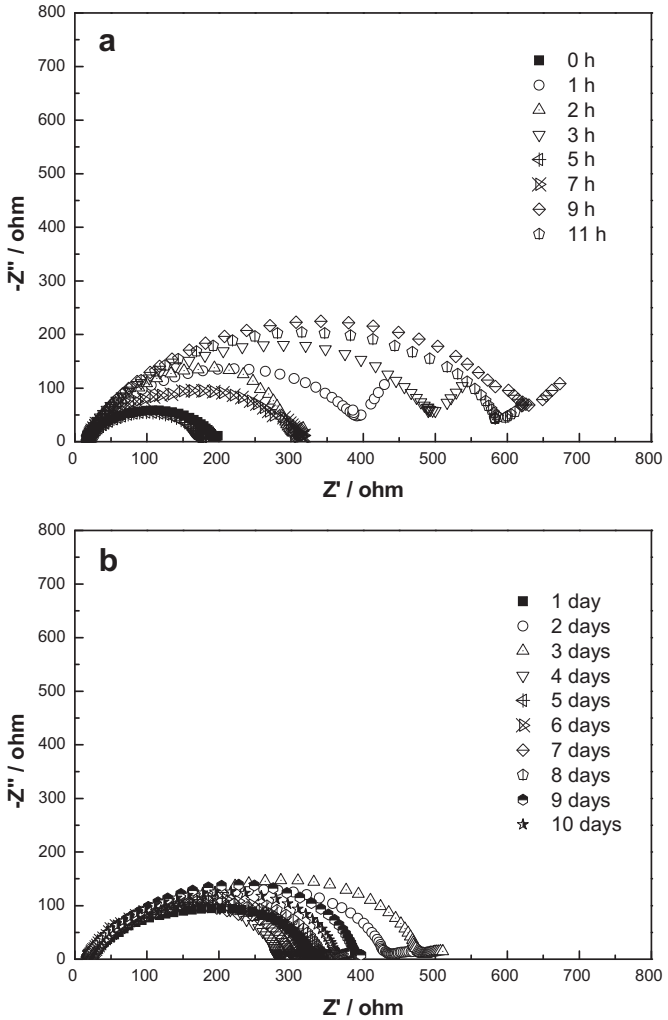

Fig. 5. Time evolution of the impedance response of a symmetrical Li/IM(2o1)1(2o2)-TFSA with 0.6 mol kg^{-1} LiTFSA electrolyte/Li cell: (a) from 0 to 11 h and (b) from 1 to 10 days.

Nevertheless, as shown in Fig. 4(a–i), the lithium redox in these nine IL electrolytes which examined by cyclic voltammogram (CV) method at room temperature could be found obviously. Taking Fig. 4(a) as example, in the first cycle for the IM112-TFSA electrolyte, the deposition of lithium was at about −0.19 V vs. Li/Li^+, and the anodic peak at about 0.34 V in the returning scan related to the dissolution of lithium. The lithium redox in this electrolyte might be caused by the formation of a passivation film on Ni electrode surface. A small cathodic peak at about 0.36 V which existed in the first cycle might be assigned to the electrochemical reduction of the IL electrolyte. The electrochemical reduction products could be assumed to be the generation of the passivation film on the Ni electrode. In addition, the cathodic peak current decreased in the rest cycles, so it could be understood that the passivation film generated in the first cycle also restrained the reduction of the IL electrolyte.

For the three IL electrolytes based on the trialkylimidazolium IL without ether group (Fig. 4(a–c)), the anodic peaks of lithium decreased with the cycle, and the decreasing of peak for IM112-TFSA and IM114-TFSA electrolytes was severe. It could also be found that the cathodic peaks of lithium in IM113-TFSA and IM114-TFSA electrolytes did not decrease obviously with the cycles, while the lithium deposition in IM112-TFSA electrolyte was restricted clearly. For the six ether-functionalized trialkylimidazolium IL electrolytes, the lithium redox behaviors of IM(2o1)21-TFSA (Fig. 4(f)) and IM(2o2)21-TFSA (Fig. 4(g)) electrolytes were close to IM113-TFSA electrolyte, and the lithium redox behaviors of IM(2o2)12-TFSA (Fig. 4(e)), IM(2o1)1(2o2)-TFSA (Fig. 4(h)) and IM(2o2)1(2o2)-TFSA (Fig. 4(i)) electrolytes were better than IM113-TFSA electrolyte. It was interesting that the redox peaks of lithium in IM(2o1)12-TFSA electrolyte (Fig. 4(d)) did not change obviously after three cycles. In these nine IL electrolytes, the lithium redox peaks in IM(2o2)1(2o2)-TFSA electrolyte were almost overlapped during the five cycles, and this IL electrolyte showed the best lithium redox behavior. These results indicated that structure of cation of IL could affect the constitution of passivation film forming on the Ni electrode, which would also affect the deposition and dissolution of lithium in IL electrolyte, and the introducing of ether group into cation of IL might be benefit for the lithium redox behavior.

Furthermore, one cathodic peak in the range from 0.8 V to 1.4 V versus Li/Li^+ and one anodic peak in the range from 0.9 V to 1.2 V versus Li/Li^+ could be found in the first cycle for the nine IL electrolytes, which might be caused by the reactions of the trace water or oxygen in IL electrolyte on Ni electrode, and these peaks disappeared or the peak currents decreased in the subsequent cycles because of the passivation film formed in the first cycle. These peaks provoked by the trace impurities, could also be found in some other IL electrolytes CV experimental results [22,65].

3.3. Chemical stabilities of the IL electrolytes against lithium metal

The chemical stabilities of these IL electrolytes against lithium metal and the interfacial characteristics between the Li metal electrode were investigated by the electrochemical impedance spectra (EIS) using the Li/IL electrolyte/Li symmetric cells. Fig. 5 illustrates the time dependence of impedance spectra for Li/IM(2o1)1(2o2)-TFSA electrolyte/Li symmetric cell under the open circuit conditions. The intercept with the real axis of the response at high frequency was assigned to electrolyte bulk resistance, and the diameter of the semicircle was related to the interfacial resistance (R_i) of the IL electrolyte/lithium metal, as explained in the literature [24,66]. For the IM(2o1)1(2o2)-TFSA electrolyte, its bulk resistance was almost unchanged during the testing period of 10 days. The R_i firstly increased and then fluctuated from 0 to 11 h, and the R_i value retained about 320 Ω after one day. The cathodic limiting potential

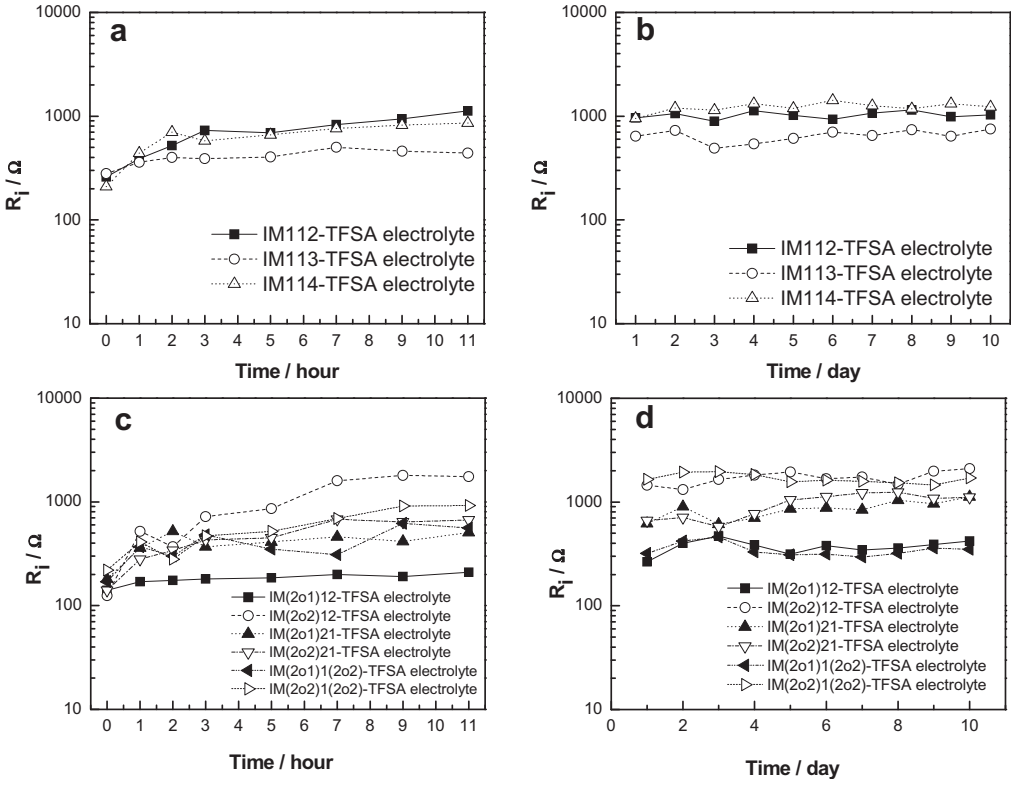

Fig. 6. Time dependence of interfacial resistance of the lithium symmetrical cells using the IL electrolytes: (a), (c) from 0 to 11 h and (b), (d) from 1 to 10 days.

of IM(2o1)1(2o2)-TFSA was about 0.6 V versus Li/Li$^+$, so it was highly possible that this IL electrolyte would continuously react with lithium metal. Fortunately, the R_i value only fluctuated a little from 1 day to 10 days and was stable at the level of 350 Ω, which could be seen in Fig. 6(d). This phenomenon might indicate that when the IL electrolyte reacted with lithium metal, a passivation layer could be produced in the meantime. The passivation layer restrained the reaction between the IL electrolyte and lithium metal, and a dynamic equilibrium state could be achieved after a period of time.

Like IM(2o1)1(2o2)-TFSA electrolyte, the time dependence of interfacial resistance (R_i) for the rest eight IL electrolytes appeared in a similar manner, as shown in Fig. 6. For the three IL electrolytes based on the trialkylimidazolium IL without ether group, their interfacial resistance values were stable in the range from 700 Ω to 1100 Ω. For the ether-functionalized IL electrolytes, IM(2o2)12-TFSA and IM(2o2)1(2o2)-TFSA electrolytes showed a stable R_i higher than 1100 Ω, IM(2o1)21-TFSA and IM(2o2)21-TFSA electrolytes also had a stable R_i in the range of 700–1100 Ω, and IM(2o1)12-TFSA and IM(2o1)1(2o2)-TFSA electrolytes owned stable R_i lower than 400 Ω. According to the above results, it could be concluded that an approximately stable state between these IL electrolytes and lithium metal could be achieved after some time, due to a passivation layer forming on the lithium metal, and the introducing of ether group into cation of IL might also have an impact on the passivation layer between IL electrolyte and lithium metal.

3.4. Charge–discharge performances of Li/LiFePO4 cells

The charge–discharge (C–D) characteristics of Li/LiFePO$_4$ cells using these nine trialkylimidazolium IL electrolytes without additive were examined at room temperature, and the cells were tested under the current rate of 0.1 C, as shown in Fig. 7. For instance, as seen in Fig. 7(a), the initial discharge capacity of the IM113-TFSA electrolyte was 126 mAh g^{-1}, and the discharge capacity increased gradually with the cycle number, which could be result from the improved wettability of the IL electrolyte to the LiFePO4 cathode during the C–D processes. The discharge capacity was stable after 20 cycles, and stabilized at the level of 140 mAh g^{-1} till the 50th cycles. The discharge capacities of M112-TFSA and IM114-TFSA electrolytes stabilized at about 130 and 135 mAh g^{-1} respectively. For the six ether-functionalized trialkylimidazolium IL electrolytes (Fig. 7(b–c)), their discharge capacities also increased with cycle number and stabilized after some cycles. The stabilized discharge capacities were close to or higher than 140 mAh g^{-1}, and IM(2o1)12-TFSA electrolyte delivered a highest capacity of 150 mAh g^{-1}. Usually, lower viscosity of IL electrolyte benefits to its wettability to electrode. However, it was easy to find from Fig. 7, that the discharge capacities reached stable after the different cycle numbers for these IL electrolytes and the electrolyte with lower viscosity did not own the smaller cycle number. For example, for IM112-TFSA, IM113-TFSA and IM114-TFSA electrolytes, they had the similar behavior of the discharge capacity with the cycle, though the viscosities of the three IL electrolytes differed obviously. In the ether-functionalized IL electrolytes, the stable cycle numbers of IM(2o2)12-TFSA and IM(2o2)21-TFSA electrolytes were about 10, and the numbers of IM(2o1)21-TFSA and IM(2o1)1(2o2)-TFSA electrolytes were about 5. So, the wettability of IL electrolyte to electrode might be related with the structure of IL besides its viscosity [67], and functionalization of cation had a chance to improve the wettability of IL electrolyte.

The rate properties of Li/LiFePO$_4$ cells are shown in Fig. 8. During the charge–discharge tests, the cells charge/discharge at 0.1 C for 20 cycles to ensure the charge/discharge capacities reach stable,

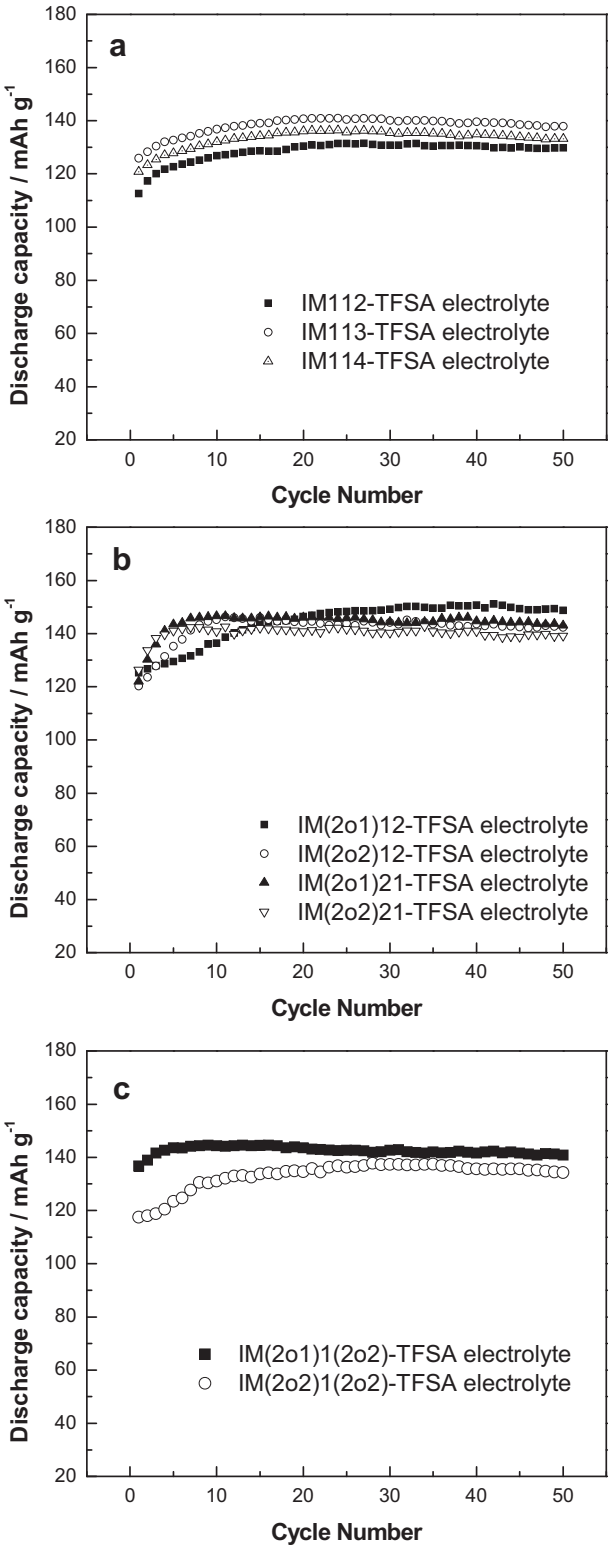

Fig. 7. Cycling performances of Li/LiFePO$_4$ cells using the IL electrolytes at 25 °C, charge–discharge current rate is 0.1 C.

then the cells charge at 0.1 C and discharge at different current rates for 4 cycles each, and the discharge capacity is normalized on the basis of discharge capacity at 0.1 C rate, which is the value after the cycle performance of cell reach stability. It was obvious that the discharge capacity decreased with the increasing discharge rate. In

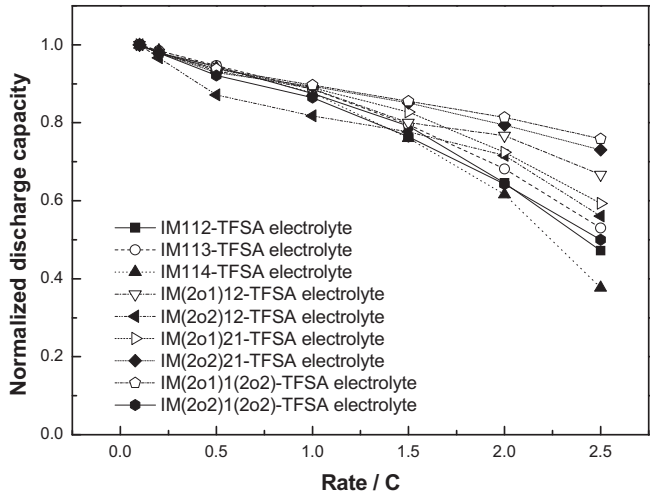

Fig. 8. Rate properties of Li/$LiFePO_4$ cells using the IL electrolytes at 25 °C. Charge current rate is 0.1 C, and discharge current rates are 0.1, 0.2, 0.5, 1.0, 1.5, 2.0 C and 2.5 C.

the three IL electrolytes based on the trialkylimidazolium IL without ether group, IM113-TFSA electrolyte delivered slightly higher discharge capacity with the increasing discharge current rate which might be attributed to its lower viscosity and higher conductivity. However, it could be found that five ether-functionalized trialkylimidazolium IL electrolytes owned better rate properties than IM113-TFSA electrolyte, and the IM(2o1)1(2o2)-TFSA electrolyte possessed the best rate properties though its viscosity and conductivity showed no advantage compared to other IL electrolytes. It was possible that the rate property was also affected by some other factors, such as the interfacial characteristics at both the LiFePO4 cathode/electrolyte and lithium metal anode/electrolyte interfaces. As shown in Fig. 9, the discharge capacity of IM(2o1)1(2o2)-TFSA electrolyte at the current rate of 1.0 C was about 128 mAh g^{-1}, which retained 90% of the capacity at the rate of 0.1 C, the capacity at 2.5 C rate was about 108 mAh g^{-1}, which still retained 76% of the capacity at the rate of 0.1 C. The results of rate performance for the nine trialkylimidazolium IL electrolytes demonstrated that ether-functionalized cation could also improve the rate performance.

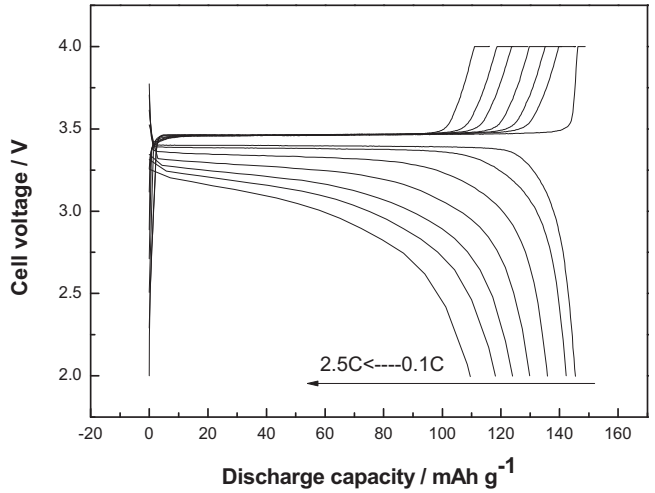

Fig. 9. Charge–discharge curves of Li/LiFePO4 cells using IM(2o1)1(2o2)-TFSA IL electrolyte at different rates at 25 °C. Charge current rate is 0.1 C, and discharge current rates are 0.1, 0.2, 0.5, 1.0, 1.5, 2.0 C and 2.5 C.

4. Conclusions

Six low-viscosity ether-functionalized ILs based on trialkylimidazolium cation with one or two ether groups and $TFSA^-$ anion were used as new electrolytes for lithium battery. Viscosity, conductivity, behavior of lithium redox, chemical stability against lithium metal, and charge–discharge characteristics of lithium battery, were investigated for these IL electrolytes and compared with the IL electrolytes based on three typical trialkylimidazolium ILs without ether group. Though the cathodic limiting potentials of the ILs were higher than 0 V versus Li/Li^+, the lithium plating and stripping on Ni electrode could be observed in these IL electrolytes. These IL electrolytes showed good chemical stability against lithium metal owning to the formation of passivation layer. Introducing of ether group into trialkylimidazolium cation can be benefit for lithium redox behavior on Ni electrode, and affect passivation layer between IL electrolyte and lithium metal. Li/$LiFePO_4$ cells using the ether-functionalized IL electrolytes without additive showed good battery performance, and IM(2o1)1(2o2)-TFSA electrolyte had better rate property.

Acknowledgments

The authors thank the Research Center of Analysis and Measurement of Shanghai JiaoTong University for the help in NMR characterization. This work was financially supports by the National Natural Science Foundation of China (Grants No. 21103108 and 21173148), and the Key Lab of Novel Thin Film Solar Cells, Chinese Academy of Sciences (Grants No. KF201110).

References

[1] J. Dupont, R.F. de Souza, P.A.Z. Suarez, Chemical Reviews 102 (2002) 3667–3692.
[2] R.D. Rogers, K.R. Seddon, Science 302 (2003) 792–793.
[3] S.A. Forsyth, J.M. Pringle, D.R. MacFarlane, Australian Journal of Chemistry 57 (2004) 113–119.
[4] H. Sakaebe, H. Matsumoto, K. Tatsumi, Electrochimica Acta 53 (2007) 1048–1054.
[5] H. Sakaebe, H. Matsumoto, K. Tatsumi, Journal of Power Sources 146 (2005) 693–697.
[6] H. Sakaebe, H. Matsumoto, Electrochemistry Communications 5 (2003) 594–598.
[7] H. Matsumoto, H. Sakaebe, K. Tatsumi, M. Kikuta, E. Ishiko, M. Kono, Journal of Power Sources 160 (2006) 1308–1313.
[8] M. Egashira, M. Nakagawa, I. Watanabe, S. Okada, J.-i. Yamaki, Journal of Power Sources 146 (2005) 685–688.
[9] M. Egashira, S. Okada, J.-i. Yamaki, D.A. Dri, F. Bonadies, B. Scrosati, Journal of Power Sources 138 (2004) 240–244.
[10] M. Egashira, M. Tanaka-Nakagawa, I. Watanabe, S. Okada, J.-i. Yamaki, Journal of Power Sources 160 (2006) 1387–1390.
[11] Y. Kobayashi, Y. Mita, S. Seki, Y. Ohno, H. Miyashiro, N. Terada, Journal of the Electrochemical Society 154 (2007) A677–A681.
[12] V. Borgel, E. Markevich, D. Aurbach, G. Semrau, M. Schmidt, Journal of Power Sources 189 (2009) 331–336.
[13] J. Jin, H.H. Li, J.P. Wei, X.K. Bian, Z. Zhou, J. Yan, Electrochemistry Communications 11 (2009) 1500–1503.
[14] A. Lewandowski, I. Acznik, A. Swiderska-Mocek, Journal of Applied Electrochemistry 40 (2010) 1619–1624.
[15] K. Matsumoto, R. Hagiwara, Y. Ito, Electrochemical and Solid-State Letters 7 (2004) E41–E44.
[16] S. Ferrari, E. Quartarone, P. Mustarelli, A. Magistris, S. Protti, S. Lazzaroni, M. Fagnoni, A. Albini, Journal of Power Sources 194 (2009) 45–50.
[17] A. Guerfi, S. Duchesne, Y. Kobayashi, A. Vijh, K. Zaghib, Journal of Power Sources 175 (2008) 866–873.
[18] J. Ranke, S. Stolte, R. Störmann, J. Arning, B. Jastorff, Chemical Reviews 107 (2007) 2183–2206.
[19] J. Dupont, J.D. Scholten, Chemical Society Reviews 39 (2010) 1780–1804.
[20] H. Saruwatari, T. Kuboki, T. Kishi, S. Mikoshiba, N. Takami, Journal of Power Sources 195 (2010) 1495–1499.
[21] I.A. Profatilova, N.-S. Choi, S.W. Roh, S.S. Kim, Journal of Power Sources 192 (2009) 636–643.
[22] M. Egashira, H. Todo, N. Yoshimoto, M. Morita, J.-I. Yamaki, Journal of Power Sources 174 (2007) 560–564.

[23] S. Seki, Y. Kobayashi, H. Miyashiro, Y. Ohno, A. Usami, Y. Mita, N. Kihira, M. Watanabe, N. Terada, Journal of Physical Chemistry B 110 (2006) 10228–10230.
[24] S. Seki, Y. Ohno, Y. Kobayashi, H. Miyashiro, A. Usami, Y. Mita, H. Tokuda, M. Watanabe, K. Hayamizu, S. Tsuzuki, M. Hattori, N. Terada, Journal of the Electrochemical Society 154 (2007) A173–A177.
[25] C. Yan, L. Zaijun, Z. Hailang, F. Yinjun, F. Xu, L. Junkang, Electrochimica Acta 55 (2010) 4728–4733.
[26] N. Jain, A. Kumar, S. Chauhan, S.M.S. Chauhan, Tetrahedron 61 (2005) 1015–1060.
[27] E.D. Bates, R.D. Mayton, I. Ntai, J.H. Davis, Journal of the American Chemical Society 124 (2002) 926–927.
[28] D. Zhao, Z. Fei, T.J. Geldbach, R. Scopelliti, P.J. Dyson, Journal of the American Chemical Society 126 (2004) 15876–15882.
[29] D. Zhao, Z. Fei, R. Scopelliti, P.J. Dyson, Inorganic Chemistry 43 (2004) 2197–2205.
[30] Q. Zhang, Z. Li, J. Zhang, S. Zhang, L. Zhu, J. Yang, X. Zhang, Y. Deng, Journal of Physical Chemistry B 111 (2007) 2864–2872.
[31] J.S. Lee, N.D. Quan, J.M. Hwang, J.Y. Bae, H. Kim, B.W. Cho, H.S. Kim, H. Lee, Electrochemistry Communications 8 (2006) 460–464.
[32] H. Matsumoto, M. Yanagida, K. Tanimoto, M. Nomura, Y. Kitagawa, Y. Miyazaki, Chemistry Letters 29 (2000) 922–923.
[33] Z.-B. Zhou, H. Matsumoto, K. Tatsumi, Chemistry – A European Journal 12 (2006) 2196–2212.
[34] Z.-B. Zhou, H. Matsumoto, K. Tatsumi, Chemistry – A European Journal 11 (2005) 752–766.
[35] Z.-B. Zhou, H. Matsumoto, K. Tatsumi, Chemistry – A European Journal 10 (2004) 6581–6591.
[36] J.H. Davis Jr., Chemistry Letters 33 (2004) 1072–1077.
[37] Z. Fei, T.J. Geldbach, D. Zhao, P.J. Dyson, Chemistry – A European Journal 12 (2006) 2122–2130.
[38] W.A. Henderson, J.V.G. Young, D.M. Fox, H.C. De Long, P.C. Trulove, Chemical Communications (2006) 3708–3710.
[39] Z. Fei, W.H. Ang, D. Zhao, R. Scopelliti, E.E. Zvereva, S.A. Katsyuba, P.J. Dyson, Journal of Physical Chemistry B 111 (2007) 10095–10108.
[40] W. Xu, L.-M. Wang, R.A. Nieman, C.A. Angell, Journal of Physical Chemistry B 107 (2003) 11749–11756.
[41] K. Tsunashima, M. Sugiya, Electrochemistry Communications 9 (2007) 2353–2358.
[42] S. Fang, L. Yang, J. Wang, M. Li, K. Tachibana, K. Kamijima, Electrochimica Acta 54 (2009) 4269–4273.
[43] H.-B. Han, K. Liu, S.-W. Feng, S.-S. Zhou, W.-F. Feng, J. Nie, H. Li, X.-J. Huang, H. Matsumoto, M. Armand, Z.-B. Zhou, Electrochimica Acta 55 (2010) 7134–7144.
[44] M. Chai, Y. Jin, S. Fang, L. Yang, S.-i. Hirano, K. Tachibana, Journal of Power Sources 216 (2012) 323–329.
[45] M. Chai, Y. Jin, S. Fang, L. Yang, S.-i. Hirano, K. Tachibana, Electrochimica Acta 66 (2012) 67–74.
[46] K. Tsunashima, F. Yonekawa, M. Sugiya, Electrochemical and Solid-State Letters 12 (2009) A54–A57.
[47] K. Tsunashima, F. Yonekawa, M. Sugiya, Chemistry Letters 37 (2008) 314–315.
[48] S. Seki, Y. Ohno, H. Miyashiro, Y. Kobayashi, A. Usami, Y. Mita, N. Terada, K. Hayamizu, S. Tsuzuki, M. Watanabe, Journal of the Electrochemical Society 155 (2008) A421–A427.
[49] S. Seki, Y. Kobayashi, H. Miyashiro, Y. Ohno, A. Usami, Y. Mita, M. Watanabe, N. Terada, Chemical Communications (2006) 544–545.
[50] S. Seki, Y. Kobayashi, H. Miyashiro, Y. Ohno, Y. Mita, A. Usami, N. Terada, M. Watanabe, Electrochemical and Solid-State Letters 8 (2005) A577–A578.
[51] S. Fang, Y. Tang, X. Tai, L. Yang, K. Tachibana, K. Kamijima, Journal of Power Sources 196 (2011) 1433–1441.
[52] S. Ferrari, E. Quartarone, P. Mustarelli, A. Magistris, M. Fagnoni, S. Protti, C. Gerbaldi, A. Spinella, Journal of Power Sources 195 (2010) 559–566.
[53] J. Pernak, K. Sobaszkiewicz, J. Foksowicz-Flaczyk, Chemistry – A European Journal 10 (2004) 3479–3485.
[54] M. Kärnä, M. Lahtinen, J. Valkonen, Journal of Molecular Structure 922 (2009) 64–76.
[55] S. Fang, Y. Jin, L. Yang, S.I. Hirano, K. Tachibana, S. Katayama, Electrochimica Acta 56 (2011) 4663–4671.
[56] S. Fang, Z. Zhang, Y. Jin, L. Yang, S.I. Hirano, K. Tachibana, S. Katayama, Journal of Power Sources 196 (2011) 5637–5644.
[57] Y. Jin, S. Fang, L. Yang, S.I. Hirano, K. Tachibana, Journal of Power Sources 196 (2011) 10658–10666.
[58] Y. Jin, S. Fang, M. Chai, L. Yang, S.-i. Hirano, Industrial & Engineering Chemistry Research 51 (2012) 11011–11020.
[59] H. Matsumoto, H. Sakaebe, K. Tatsumi, Journal of Power Sources 146 (2005) 45–50.
[60] Y. Saito, T. Umecky, J. Niwa, T. Sakai, S. Maeda, Journal of Physical Chemistry B 111 (2007) 11794–11802.
[61] T. Frömling, M. Kunze, M. Schönhoff, J. Sundermeyer, B. Roling, Journal of Physical Chemistry B 112 (2008) 12985–12990.
[62] K. Hayamizu, S. Tsuzuki, S. Seki, Y. Ohno, H. Miyashiro, Y. Kobayashi, Journal of Physical Chemistry B 112 (2008) 1189–1197.
[63] M.J. Monteiro, F.F.C. Bazito, L.J.A. Siqueira, M.C.C. Ribeiro, R.M. Torresi, Journal of Physical Chemistry B 112 (2008) 2102–2109.
[64] M.J. Monteiro, F.F. Camilo, M.C.C. Ribeiro, R.M. Torresi, Journal of Physical Chemistry B 114 (2010) 12488–12494.
[65] M. Moshkovich, Y. Gofer, D. Aurbach, Journal of the Electrochemical Society 148 (2001) E155–E167.
[66] A. Fernicola, F. Croce, B. Scrosati, T. Watanabe, H. Ohno, Journal of Power Sources 174 (2007) 342–348.
[67] C.S. Stefan, D. Lemordant, B. Claude-Montigny, D. Violleau, Journal of Power Sources 189 (2009) 1174–1178.